Radical Cation of 2,5-Dimethyl-2,4-hexadiene: Resonance Raman Spectrum and Molecular Orbital Calculations

Gurusamy Balakrishnan, Jesper F. Offersgaard,† and Robert Wilbrandt*

Condensed Matter Physics and Chemistry Department, Risø National Laboratory, 4000 Roskilde, Denmark

Received: June 22, 1999; In Final Form: October 7, 1999

The radical cation of 2,5-dimethyl-2,4-hexadiene (tetramethylbutadiene, TMB) is studied experimentally by time-resolved resonance Raman (RR) spectroscopy and theoretically by ab initio and density functional theory calculations (UHF, UBLYP, UB3LYP, and CASSCF using the 6-31G(d) basis set). The radical cation is produced in solution at room temperature by laser flash photolysis, and its RR spectrum is excited in resonance with the optically allowed, strong, second electronic $2^2A_u \leftarrow 1^2B_g$ transition around 365 nm. Calculated transition energies and oscillator strengths agree qualitatively well with reported absorption data. On the basis of the molecular orbital calculations carried out, the observed RR spectrum is assigned to a mixture of s-trans and gauche conformers, the first being strongly predominant. A lower limit of 42 kJ mol^{-1} is estimated for the torsional energy barrier between the two conformers. Equilibrium geometries and electronic transitions are discussed.

1. Introduction

Studies on the radical cations of polyenes are of general interest toward the understanding of the mechanism of photoconductivity in organic conducting polymers and are of fundamental importance to understand the charge redistribution and structural changes upon oxidation. The spectroscopy of polyenes has consequently been an active field of research for the past decades.[1−9] Previously, our group reported studies of a series of butadiene[10−12] and its monomethyl substituted[10,13,14] radical cations. The present work is an extension to hexadiene to further understand the influence of methyl groups on the carbon skeleton and associated structural changes.

Most of the radical cations of short polyenes are known to decay very fast (<50 ns) and to have too high ionization potentials to be generated photochemically in solution by means of currently available laser sources. Therefore, in our previous resonance Raman (RR) studies, they were generated by γ-irradiation at low temperature in Freon matrices. Although the Freon matrix is a useful spectroscopic medium, its strong UV absorption prevented the RR characterization of diene radical cations in resonance with their short wavelength electronic transitions around 300 nm. The radical cation of 2,5-dimethyl-2,4-hexadiene (tetramethylbutadiene, TMB), however, provides an opportunity for UV RR examination, as it is produced[15] by laser flash photolysis at 248 nm in solution, having a lifetime of $>5\,\mu$s. In the present study, the RR spectrum of TMB, excited in resonance with the strong electronic absorption band around 360 nm, is reported. The spectrum is interpreted on the basis of *ab initio* and density functional theory (DFT) calculations. To our knowledge, this is the first resonance Raman report on the radical cation of TMB.

The molecular, electronic, and vibrational structure of ground and excited states of neutral TMB has been studied thoroughly by both experimental and theoretical methods.[16−18] In previous work, we also have reported the time-resolved resonance Raman (TRRR) spectrum and Quantum Chemical Force Field (QCFF/PI) theoretical studies on the triplet excited state of TMB in acetonitrile.[16,17] As shall be discussed below, in view of the present results on the radical cation, it seems most likely that the RR spectrum previously assigned to the lowest excited triplet state, in fact was due to the radical cation of TMB.

2. Materials and Methods

2.1. Materials. *s-trans*-2,5-Dimethyl-2,4-hexadiene (tetramethylbutadiene, TMB) and 1,4-diazabicyclo[2.2.2]octane (DABCO) were obtained from Aldrich and used as received. Spectral grade CH_3CN (Merck) and CD_3CN (D, 99.8%, Cambridge Isotope Laboratories, Inc., CIL) were also used as received.

2.2. Experimental Methods. The radical cation of TMB was produced by laser flash photolysis in solution at room temperature, as described in the literature.[15] TMB (1.6×10^{-4} M in aerated acetonitrile) was oxidized to its radical cation by means of direct photoionization at 248 nm (Lambda Physik LPX 220i Excimer laser, KrF, 6.0 mJ, 20 ns pulses). The RR spectrum of the transient radical cation in the region 200−3000 cm^{-1} was excited 70−100 ns after the photolyzing light pulse, at a wavelength of 360 nm (Continuum, Sunlite OPO, 2.0 mJ, 5 ns). The OPO (optical parametric oscillator) was pumped by the 355 nm output from a Nd:YAG laser (Continuum, Powerlite PL9010). The excimer pump and OPO probe lasers were operated at 10 Hz, and the time delay between the pulses was controlled by a time delay generator (Stanford DG535). Sample solutions were contained in a rotating cylindrical quartz cell of 3 cm inner diameter. The scattered light was collected at a right angle to the laser beam, passed through a band-pass filter (Schott WG 320) and a polarization scrambler and dispersed in a single monochromator (Jobin Yvon- T64000) equipped with a 2400 grooves/mm grating. A back illuminated liquid N_2 cooled charge coupled device CCD (Princeton Instruments) with 1100×330 pixels was used as the multichannel detector. The wavenumber scale was calibrated using cyclohexane Raman bands as a

* Author to whom correspondence should be addressed. Present address: Bornholms Amtsgymnasium, Soeborgstraede 2, DK 3700 Roenne, Denmark. E-mail: robert-wilbrandt@bornholm-gym.dk.

† Present address: DELTA Light & Optics, Hjortekærsvej 99, DK-2800 Lyngby, Denmark.

10.1021/jp992071u CCC: $18.00
Published on Web 11/24/1999

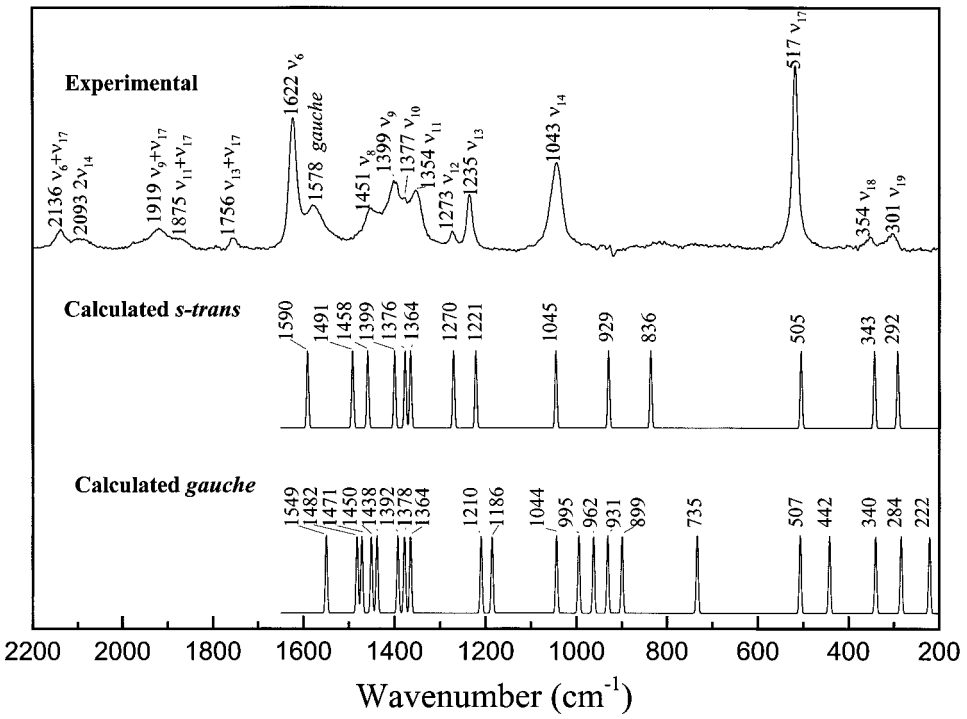

Figure 1. Experimental resonance Raman spectrum of the radical cation of 2,5-dimethyl-2,4-hexadiene, together with the UBLYP/6-31G(d) calculated totally symmetric harmonic frequencies of its two conformers.

reference. Each sample was exposed to 1200 laser pulses, and spectra from three samples were averaged. The final spectra were obtained after subtraction of both neutral TMB and solvent bands. They were not corrected for the absorption of the band-pass filter, the absorption of the sample, and the wavelength dependence of the sensitivity of our detection system. Optical absorption spectra of the solution before and after each TRRR measurement were compared, and no detectable photoproducts were observed. Neither were any new Raman bands from photoproducts observed after the transient experiment.

2.3. Computational Methods. Molecular orbital calculations were performed either by ab initio Hartree−Fock (HF) or density functional theory (DFT)[19−21] methods using BLYP (using the Becke exchange and the Lee, Yang, and Parr correlation functionals) and B3LYP (the Becke three-parameter hybrid method that uses the same LYP correlation functional) functionals as contained in the Gaussian suite of programs.[22] Restricted closed-shell and unrestricted open-shell wave functions were employed for the neutral and radical cation, respectively. Furthermore, properties of ground and excited states of the radical cation of TMB were evaluated by CASSCF (Complete Active Space Self-Consistent Field) methods using the DALTON program.[23] The excited state, corresponding to the resonant optical transition, was identified based on the results of multiconfigurational linear response calculations of transition energies and oscillator strengths at the ground-state optimized geometry. The geometry optimization was carried out in C_{2h} point group for neutral and C_{2h}, C_i, and C_2 point groups for the radical cation of *s-trans*-TMB. In the case of gauche-TMB, both neutral and radical cation were optimized in C_2 point group. Vibrational frequencies were calculated at the optimized geometries using analytical derivative techniques. In the CASSCF calculations on the radical cation, three electrons were correlated in four π orbitals (two a_u, and two b_g orbitals) in C_{2h} symmetry, whereas the CASSCF calculations on the neutral TMB involved four electrons in four π orbitals. The standard 6-31G(d) basis set was used throughout.

The spin contamination due to the use of unrestricted wave functions was found to be minor. For example, the expectation value, $\langle S^2 \rangle$, obtained from the UBLYP (U for unrestricted) and UB3LYP calculations were found to be 0.7531 and 0.7593, respectively, against the expected value of 0.75 for the doublet radical cation. However, in the case of UHF calculations, this value was slightly higher (0.8428), indicating that some spin contamination is present in this case.

3. Resonance Raman Spectrum of $TMB^{\bullet+}$

The radical cation of TMB ($TMB^{\bullet+}$) was generated by means of direct photoionization of TMB (1.6×10^{-4} M) in aerated acetonitrile solution. The electronic absorption spectrum of $TMB^{\bullet+}$ under similar experimental conditions (with 266 nm as the photolyzing pulse) has been reported in the literature.[15] It contains one strong band at 365 nm ($\epsilon = 11\,700$ M^{-1} cm^{-1}) and a weaker and broader band in the visible (400−580 nm) region. In the present work, 360 nm was selected as the probe wavelength to record the resonance enhanced Raman spectrum of $TMB^{\bullet+}$. The observed spectrum is shown Figure 1. The spectral region between 200 and 2200 cm^{-1} contains a total of 17 Raman bands, and four weak bands at 2436, 2581, 2666, and 2864 cm^{-1} were additionally observed in the spectral region of 2200−3000 cm^{-1} (not included in Figure 1). All vibrational bands were observed to decay with the same rate constant (half-life, ∼5.0 μs) indicating that the observed resonance Raman spectrum corresponds to a single transient species, namely the radical cation. To confirm the identity of the radical cation, additional experiments in the presence of 1.0 mM DABCO were carried out. It was observed that the transient species, arising from photolysis of TMB, was quenched completely in the presence of DABCO. As DABCO is known for its low oxidation potential, the quenching is explained by electron transfer from DABCO to the radical cation of TMB. The complete absence of transient bands in the presence of DABCO indicates that the observed transient indeed is the radical cation of TMB and, in

TABLE 1: Calculated Total Energies (in Hartree) and the Energy Differences (Δ, in kJ mol^{-1})[a] of the Neutral and Radical Cation of 2,5-Dimethyl-2,4-hexadiene Using the Standard 6-31G(d) Basis Set

	UHF	Δ_1	UBLYP		UB3LYP	Δ_1	CASSCF	Δ_1
			Neutral					
C_{2h}-trans[b]	−311.0691225		−313.0668632		−313.2656523		−311.1226851	
C_2-gauche[b]	−311.0657303	8.91	−313.0599920	18.04	−313.2598405	15.26		
			Radical Cation					
C_2-gauche[b]	−310.8258139	44.94	−312.8018706	38.30	−312.9906786	39.28		
		Δ_2		Δ_2		Δ_2		Δ_2
C_{2h}-trans[c]	−310.8429292		−312.8164601		−313.0056399		−310.8604735	
C_2-trans[b]	−310.8430333	−0.27	−312.8164935	−0.09	−313.0056884	−0.13		
C_i-trans[b]	−310.8430178	−0.23	−312.8165028	−0.11	−313.0056956	−0.15	−310.8605379	−0.17

[a] Δ_1, the diffence in energy of gauche C_2 with respect to trans C_{2h} structure. Δ_2, the diffence in energy of trans C_2 and C_i structures with respect to trans C_{2h} structure. [b] No imaginary frequencies. [c] Two imaginary frequencies.

TABLE 2: Calculated Bond Lengths (in Å), Bond and Dihedral Angles (in Degrees) of Neutral and the Radical Cation of 2,5-Dimethyl-2,4-hexadiene Using Standard 6-31G(d) Basis Set with Four Different Methods[a]

	s-trans C_{2h}									gauche C_2					
	neutral, ^1A_g ground state				radical cation, ^2B_g ground state				2^2A_u state	^1A neutral, ground state			radical cation, ^2A ground state		
parameters	HF	CASSCF	BLYP	B3LYP	UHF	CASSCF	UBLYP	UB3LYP	CASSCF[b]	HF	BLYP	B3LYP	UHF	UBLYP	UB3LYP
C_1C_2	1.509	1.511	1.518	1.508	1.499	1.499	1.500	1.492	1.483	1.510	1.519	1.509	1.500	1.502	1.493
C_2C_3	1.331	1.351	1.365	1.352	1.394	1.397	1.415	1.404	1.462	1.327	1.360	1.348	1.393	1.412	1.401
		(1.344)	(1.353)			(1.387)	(1.399)				(1.352)			(1.398)	
C_3C_4	1.468	1.467	1.457	1.454	1.391	1.393	1.411	1.401	1.436	1.483	1.477	1.472	1.399	1.422	1.411
		(1.465)	(1.461)			(1.398)	(1.421)				(1.476)			(1.431)	
C_5C_8	1.509	1.510	1.517	1.508	1.498	1.499	1.500	1.491	1.482	1.508	1.517	1.508	1.498	1.501	1.492
$C_1C_2C_3$	120.6	120.4	120.5	120.6	119.3	119.3	119.0	119.1	119.5	121.0	120.7	120.8	118.7	118.6	118.7
$C_1C_2C_7$	113.7	114.1	114.5	114.4	115.6	115.6	116.8	116.5	119.7	114.6	115.3	115.2	115.6	116.8	116.5
$C_7C_2C_3$	125.7	125.4	125.0	125.2	125.1	125.1	124.2	124.4	120.7	124.4	124.4	124.0	125.3	124.4	124.8
C_3C_4H	127.2	127.0	127.5	127.3	125.2	125.2	125.8	125.5	119.5	128.4	129.1	128.7	131.7	132.0	131.6
$C_3C_4C_5$	116.2	116.5	116.4	116.4	118.6	119.2	118.3	118.5	123.9	114.2	114.2	114.4	113.5	113.4	113.4
HC_4C_5	116.6	116.5	116.2	116.3	116.1	115.9	115.8	116.0	116.6	117.4	116.5	116.8	114.5	114.4	114.5
$C_1C_2C_3C_4$	180.0	180.0	180.0	180.0	180.0	180.0	180.0	180.0	180.0	178.9	180.1	180.0	174.4	173.0	173.6
$C_2C_3C_4C_5$	180.0	180.0	180.0	180.0	180.0	180.0	180.0	180.0	180.0	64.1	54.7	56.0	31.3	32.8	32.7
$C_3C_4C_5C_8$	0.0	0.0	0.0	0.0	0.0	0.0	0.0	0.0	0.0	0.1	2.5	1.9	12.2	12.8	12.4

[a] Values given in parentheses correspond to 1,3-butadiene taken from ref 12. [b] In C_i point group, two imaginary frequencies.

particular, that the observation of Raman bands from the lowest triplet excited state of TMB can be ruled out.

As discussed in the next section, all the calculations suggest the presence of a totally symmetric a_g mode (ν_{15}) in the region 893−923 cm^{-1}, which is not observed experimentally in CH_3-CN. To avoid possible overlap with and masking by the strong solvent band of CH_3CN at 921 cm^{-1}, we did experiments under similar conditions in CD_3CN, which has no Raman band in this region. The spectra in both solvents were very similar, and no additional bands were observed in CD_3CN. All experimentally observed resonance Raman bands could be unambiguously assigned to calculated normal modes of TMB$^{\bullet+}$ as described below.

4. Calculations

While geometry optimizations of *s-trans*-TMB and its radical cation resulted in planar skeleton structures, as discussed in the following section, attempts to optimize *s-cis*-TMB and its radical cation in the planar C_{2v} point group always ended with nonplanar gauche structures. Calculated dihedral angles (butadiene part) close to ∼60° and ∼30° for neutral and radical cation, respectively, suggested the absence of a stable planar cis conformer. Therefore, for the cis form, only gauche structures will be presented. It should be noted that, as observed from our earlier studies on other radical cations of short polyenes, the distinction between single and double bonds is meaningless. Calculated energies and geometries for neutral TMB and its radical cation are listed in Tables 1 and 2, respectively. The molecular structure of *s-trans*- and gauche-TMB and the numbering of atoms used in this paper are shown in Figure 2.

4.1. Geometries. *4.1.1. Neutral TMB.* For *s-trans*-TMB, all calculations result in an optimized C_{2h} geometry. For gauche-TMB, a C_2 geometry with a slightly elongated central C_3C_4 bond and a dihedral angle in the range 54.7−64.1°, depending on calculation method, is predicted. As the calculations result in no imaginary frequencies, these calculated structures for the neutral species are real minima on the potential energy surfaces. The energy of the gauche form is calculated to be moderately (8.9−18.0 kJ mol^{-1}) higher than that of the s-trans form.

4.1.2. Radical Cation of TMB. 4.1.2.1. s-Trans- TMB$^{\bullet+}$. The structural optimization of *s-trans*-TMB$^{\bullet+}$ in the C_{2h} point group resulted in two (a_u,b_u) imaginary frequencies. From the visual inspection of the normal mode displacements, it was seen that these two imaginary frequencies corresponded to methyl distortions and did not contain any significant contribution from the main carbon skeleton. A further optimization with reduced symmetry resulted in structures of C_2 and C_i point groups, neither of which showed any imaginary frequencies. The energy differences of these C_2 and C_i structures, relative to the C_{2h} geometry, were very small (0.09−0.27 kJ mol^{-1}), indicating a very shallow potential along these methyl deformational coordinates. Also the structural parameters, such as bond lengths and bond angles, obtained were identical for all the above three structures except for small variations (<1°) in dihedral angles. To illustrate these findings, the relevant bond and dihedral angels obtained from UBLYP calculations (as a representative case)

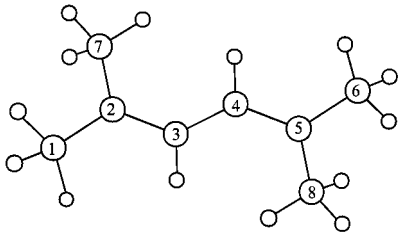

(a) s-*trans*-2,5-dimethyl-2,4-hexadiene

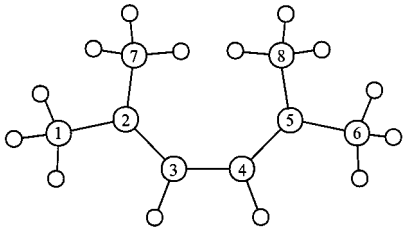

(b) *gauche*-2,5-dimethyl-2,4-hexadiene

Figure 2. Schematic drawings of the s-trans and gauche conformers of 2,5-dimethyl-2,4-hexadiene showing the numbering scheme used for geometry data.

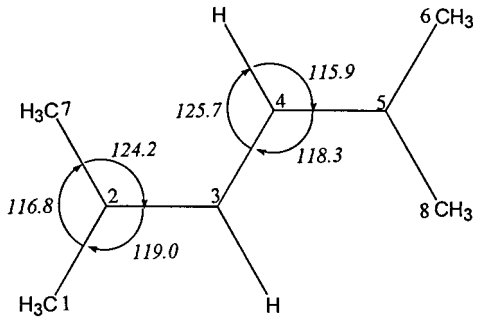

$C_1C_2C_3C_4$ 179.5 (179.4)
$C_2C_3C_4C_5$ 179.2 (180.0)
$C_3C_4C_5C_8$ 0.9 (0.8)

Figure 3. Calculated bond and dihedral angles of *s-trans*-2,5-dimethyl-2,4-hexadiene radical cation in the C_2 point group using UBLYP/6-31G(d) methods. Values in parentheses correspond to the C_i point group (see the text for more details).

are shown in Figure 3 for C_i and C_2 point groups. Only one set of bond angles is given, as C_i and C_2 point groups yielded identical values. In view of the small structural and energetic differences among the three structures, we decided to use the calculated C_{2h} geometry as a basis for frequency calculations. We believe that such a restriction to the C_{2h} point group does not affect the main conclusions with respect to vibrational analysis.

The calculated structural parameters such as bond lengths and bond angles corresponding to the main carbon skeleton are given in Table 2 for both the neutral and the radical cation of *s-trans*-TMB (in the C_{2h} point group). Similar calculations were extended to gauche-TMB (in the C_2 point group) and its radical cation. Because of severe SCF convergence problems, we restricted our CASSCF calculations to only the planar *s-trans*-TMB and its radical cation.

4.1.2.2. gauche-TMB$^{\bullet+}$. The calculated geometries of the radical cation in a gauche conformation in the C_2 point group were found to correspond to real minima for all calculation methods used. The torsional angle of the central CC bond becomes smaller (around 30°) in the case of the radical cation as compared to the neutral (around 60°), which is a consequence of the change in the bond lengths of the main carbon skeleton. The gauche form of the radical cation was calculated to be substantially higher (38.3−44.9 kJ mol^{-1}) in energy than the s-trans form.

TABLE 3: Calculated Vertical Transition Energies and Oscillator Strengths of the Radical Cation of *s-trans*-2,5-Dimethyl-2,4-hexadiene Using CASSCF/6-31G(d) Linear Response Calculations within the C_{2h} Point Group

ex. states		energy			osc. str
sym	no.	eV	cm^{-1}	nm	length
A_u	1	2.44	19674	508	0.0340
	2	3.26	26290	380	0.6591
B_g	1	5.75	46471	215	
	2	6.60	53338	187	
A_g	1	5.96	48100	208	
	2	6.36	51382	195	
B_u	1	6.64	53609	186	0.0002
	2	7.50	60530	165	0.0096

TABLE 4: Observed and Calculated Vibrational Frequencies (cm^{-1}) of the Radical Cation of *s-trans*-2,5-Dimethyl-2,4-hexadiene within the C_{2h} Point Group using the Standard 6-31G(d) Basis Set

mode	UHF[a]	UBLYP	UB3LYP[b]	CASSCF[c]	expt
ν_6	1625	1590	1607	1572	1622
ν_7	1463	1491	1484	1414	
ν_8	1436	1458	1452	1397	1451
ν_9	1396	1399	1400	1390	1399
ν_{10}	1383	1376	1376	1349	1377
ν_{11}	1360	1364	1363	1338	1354
ν_{12}	1257	1270	1268	1212	1273
ν_{13}	1196	1221	1223	1155	1235
ν_{14}	930	1045	1046	993	1043
ν_{15}	923	929	926	893	
ν_{16}	801	836	836	774	
ν_{17}	481	505	502	464	517
ν_{18}	328	343	340	316	354
ν_{19}	279	292	290	269	301
rms	33.7	12.2	7.8	21.8	

[a] Scaled by 0.89. [b] Scaled by 0.97. [c] Scaled by 0.86.

4.2. Excited States and Electronic Transitions. The calculated energies (CASSCF, linear response calculations) of the two lowest excited electronic states of each symmetry within the C_{2h} point group of *s-trans*-TMB$^{\bullet+}$, calculated at the ground-state geometry, are given in Table 3, together with calculated oscillator strengths for the transitions from the ^2B_g ground state. On the basis of these results, the UV transition observed at 365 nm is assigned to the 2 $^2A_u \leftarrow 1\ ^2B_g$ transition, calculated at 3.26 eV (380 nm), in qualitatively good agreement with experiment.

A CASSCF optimization and force field calculation of the excited state (2 ^2A_u) yielded seven imaginary frequencies within the C_{2h} point group. Upon reduction of symmetry to C_i, two imaginary frequencies remained and further reduction to C_2 yielded one imaginary frequency. The C_i structure is listed in Table 2.

4.3. Vibrational Frequencies. The vibrational frequencies corresponding to the totally symmetric modes of *s-trans*-TMB$^{\bullet+}$ in the C_{2h} point group, calculated using different methods such as UHF, UBLYP, UB3LYP, and CASSCF are given in Table 4. The calculated (UBLYP) Raman frequencies (totally symmetric modes only) of the s-trans and gauche conformers of TMB$^{\bullet+}$ are also shown as stick spectra in Figure 1.

5. Discussion

5.1. Molecular and Electronic Structure of TMB and TMB$^+$. The stable neutral 2,5-dimethyl-2,4-hexadiene is observed to exist in a planar C_{2h} s-trans conformation, whereas, in the case of the cis conformer, the calculation results in a nonplanar C_2 gauche conformation. The dihedral angle defined by the two ethylene moieties ranges from 56° to 64° from different calculations as shown in Table 2. Such a nonplanar gauche structure was previously reported for monomethyl-substituted 1,3-butadienes, namely the *trans*- and *cis*-1,3-pentadienes.[13] The total energy difference of 18.03 kJ mol^{-1} between s-trans and gauche suggests a true value rather close to that reported[13] for *cis*-pentadiene (16.30 kJ mol^{-1}). The calculated bond lengths and angles of the s-trans and gauche conformers of TMB are very similar, except for the central C−C bond. The calculated (BLYP) central C−C bond is found to be longer in the gauche (1.477 Å) compared to the s-trans (1.457 Å) conformer. This difference in bond length and the dihedral angle suggest that the steric strain introduced by the methyl groups plays a major role in determining the stable conformation of the molecule.

In the case of the radical cation, as found for butadiene and its monomethyl derivatives, the bond length alternation between formal C−C and C═C bond decreases substantially compared to the neutral. However, the calculated differences (as seen from Table 2), are much smaller (about 3−4 pm for the s-trans conformer) than observed for the radical cation of butadiene and its monomethyl derivatives, indicating that methyl substitution plays a significant role in further reducing bond length alternation. However, in the case of the gauche conformer, due to steric interaction, the bond length alternation is somewhat higher than for the s-trans conformer. It is also interesting to note that, for the gauche conformer, upon oxidation, the methyl groups are moving away from the plane defined by the central butadiene moiety. The methyl group trans to vinyl hydrogen changes by ∼10°, while the one cis to vinyl hydrogen changes by about ∼5°. All these observations together suggest that methyl substitution introduces more complicated effects than what one would expect based on simple considerations of ionization and extended resonance effect of the positive charge over the terminal methyl groups. The influence of tetramethyl substitution seems to be more pronounced in the case of the radical cation as compared to the neutral. For example, based on UBLYP calculations, the change in central C−C bond length when going from *s-trans*-butadiene[12] to *s-trans*-TMB is only −4 pm, whereas the value corresponding to the radical cation is −10 pm. A similar comparison for the C═C bond yields +12 and +16 pm for the neutral and radical cation, respectively.

Comparison between the CASSCF geometry of the 2^2A_u excited state with the ground state of s-*trans*-TMB$^{+\bullet}$ suggests that the excited state has intermediate character between the ground state of the neutral and the radical cation. For example, the bond lengths of the formal C═C and C−C (central) bonds are intermediate between the ground state of neutral and radical cation. Other noticeable differences found on going from ground to the second excited state are changes in bond angles, such as $C_1C_2C_7$ (+4.1°), $C_7C_2C_3$ (−4.4°), C_3C_4H (−5.7°), and $C_3C_4C_5$ (+5.7°). A visualization of these overall changes suggests that the excited state distorts along the CC stretching and in-plane CCC/CCH bending coordinates. These predictions are in line with our experimental observation of strong resonance-enhanced bands at 1622 and 517 cm^{-1}, which will be discussed in detail in the next section.

TABLE 5: Observed and Calculated [UB-LYP/6-31G(d)] Vibrational Frequencies (cm^{-1}) and Potential Energy Distributions (PED in %) of the Totally Symmetric (a_g) normal Modes of the *s-trans*-2,5-Dimethyl-2,4-hexadiene Radical Cation

mode	obsd	calcd	assignment and PED[a]
ν_6	1622	1590	$\nu_{C=C}$, 32; δ_{CCH}, 30; ν_{C-C}, 24
ν_7		1491	δ_{CCH},46(me); ν_{C-C}, 24
ν_8	1451	1458	δ_{CCH},48(me); ν_{C-C}, 10
ν_9	1399	1399	δ_{CCH}, 51(me); ν_{C-C}, 16; $\nu_{C=C}$, 12
ν_{10}	1377	1376	δ_{CCH},44(me); ν_{C-Cme}, 23
ν_{11}	1354	1364	δ_{CCH},52(me); ν_{C-C}, 18
ν_{12}	1273	1270	δ_{CCH},35; ν_{C-C}, 24; δ_{CCC}, 10
ν_{13}	1235	1221	ν_{C-Cme}, 48; δ_{CCH},28; ν_{C-C}, 16
ν_{14}	1043	1045	δ_{CCH},62(me); ν_{C-Cme}, 13
ν_{15}		929	δ_{CCH},65(me); ν_{C-Cme}, 21
ν_{16}		836	ν_{C-Cme}, 72; δ_{CCC}, 15
ν_{17}	517	505	δ_{CCC}, 33; ν_{C-Cme}, 15; τ_{CCCH}, 20
ν_{18}	354	343	τ_{CCCH}, 36; δ_{CCC}, 25
ν_{19}	301	292	δ_{CCC}, 54; τ_{CCCH}, 12

[a] PEDs are obtained in internal coordinates using the NMODE[28] program. Only the contributions greater than 10% are given in the table: ν, stretch; δ, bend; τ, torsion.

The neutral *s-trans*-TMB corresponds to a ^1A_g state within the C_{2h} point group. Upon photoionization, the state symmetry changes to ^2B_g. For the radical cation of s-*trans*-TMB, the lowest two allowed electronic transitions (see Table 3) calculated using CASSCF methods are the $1\ ^2A_u \leftarrow 1\ ^2B_g$ and $2\ ^2A_u \leftarrow 1\ ^2B_g$ transitions. The corresponding energies of 2.44 eV (508 nm) and 3.26 eV (380 nm) are in good agreement with the experimentally reported absorption maxima of 400−580 and 365 nm, respectively.[15] The predicted relative oscillator strength of the higher energy transition is about 20 times larger than that of the lower energy transition which is in qualitatively good agreement with the reported absorption spectrum in the literature.[15]

5.2. Vibrational Assignments. A satisfactory vibrational assignment of neutral s-*trans*-TMB based on experimental and theoretical data is available from the literature.[16−18] Therefore, the present work is concerned only with the radical cation of TMB.

The experimentally observed resonance Raman frequencies, normal mode descriptions, and assignments for *s-trans*-TMB$^{\bullet+}$ are given in Table 5 along with the calculated frequencies based on the UBLYP method. The potential energy distribution in internal coordinates was obtained from the force field and displacements of UBLYP calculated data using the NMODE program.[28] The normal mode displacements of the 14 totally symmetric (five ν_{C-H} modes are not included) modes are shown in Figure 4.

In the C_{2h} molecular framework, the irreducible representations of the vibrational modes of TMB$^{\bullet+}$ are divided as 19 a_g + 11 b_g + 12 a_u + 18 b_u. The a_g and b_g modes are expected to be Raman active and the a_u and b_u modes are expected to be IR active. In the absence of vibronic coupling or changes of the point group upon excitation, only the 19 totally symmetric a_g modes are expected to be active in the resonance Raman spectrum via the Franck−Condon scattering mechanism. Of the 19 a_g modes, only 14 are in the region 200−1800 cm^{-1} and will be discussed here. The remaining five modes corresponding to ν_{C-H} frequencies will not be discussed since no experimental data are available.

The assignment of the observed RR spectrum is carried out in the following way. First, on the basis of calculated frequencies, vibrational bands are assigned to totally symmetric modes (fundamentals, overtones and combinations) of *s-trans*-TMB$^{\bullet+}$.

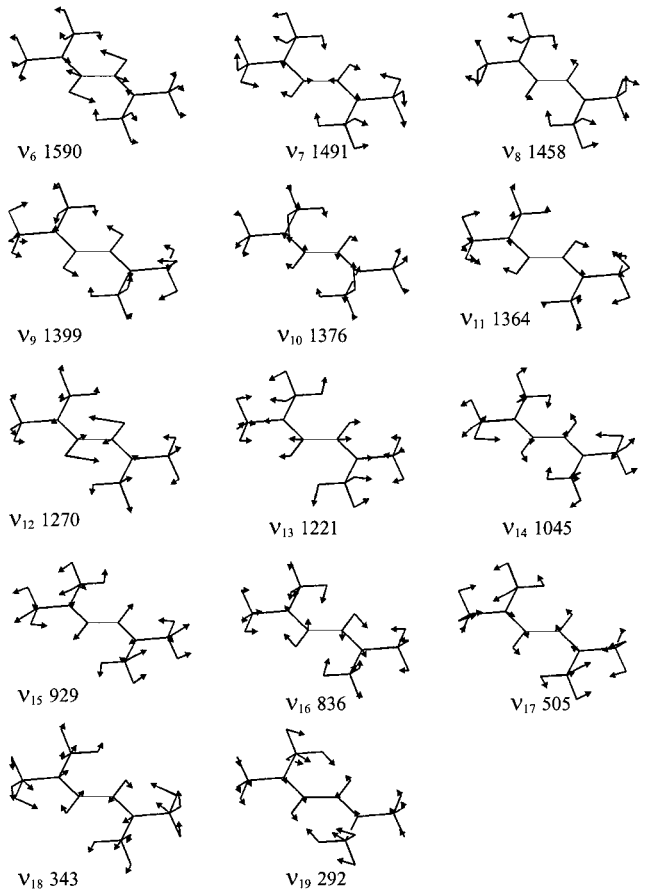

Figure 4. Normal mode displacements of the totally symmetric modes (ν_{C-H} stretching modes are excluded) of *s-trans*-2,5-dimethyl-2,4-hexadiene radical cation obtained using UBLYP/6-31G(d) methods.

Then, an attempt will be made to assign yet unassigned bands to the gauche conformer. (Calculated frequencies in the following are those from UBLYP calculations as depicted in Figure 1 and listed in Table 5.) The 11 bands in the region of 200−1700 cm^{-1} are assigned to fundamentals as follows. The band observed at 1622 cm^{-1} corresponds to the CC stretching mode ν_6 (calculated at 1590 cm^{-1}). The four bands at 1451, 1399, 1377, and 1354 cm^{-1} are assigned to modes with major contributions from methyl deformation (ρ_{CH3}) calculated at 1458 (ν_8), 1399 (ν_9), 1376 (ν_{10}), and 1364 (ν_{11}) cm^{-1}. The bands observed at 1273 and 1235 cm^{-1} are assigned to strongly coupled modes corresponding to the C−CH_3, C═C, and central C−C stretching modes. The corresponding calculated values are 1270 (ν_{12}) and 1221 (ν_{13}) cm^{-1}. The broad band observed at 1043 cm^{-1} is assigned to the calculated ν_{14} mode at 1045 cm^{-1}. It may, however, also contain a contribution from the first overtone of the observed 517 cm^{-1} band, contributing to the large width of the 1043 cm^{-1} band. The low-frequency bands observed at 517, 354, and 301 cm^{-1} are assigned to the calculated modes at 505 (ν_{17}), 343 (ν_{18}), and 292 (ν_{19}) cm^{-1}.

Remaining bands above 1700 cm^{-1} are assigned to various combinations and overtones such as 1756, 1875, 1919, 2093, and 2136 cm^{-1} to $\nu_{13} + \nu_{17}$, $\nu_{11} + \nu_{17}$, $\nu_9 + \nu_{11}$, $2\nu_{14}$, $\nu_6 + \nu_{17}$, respectively. Other weaker combination bands observed in the higher wavenumber region are 2436 ($\nu_9 + \nu_{14}$), 2581 ($\nu_{11} + \nu_{13}$), 2666 ($\nu_6 + \nu_{16}$), and 2864 ($\nu_6 + \nu_{13}$) cm^{-1}.

From this analysis, only one band, observed at 1578 cm^{-1}, is left unassigned. As observed for butadiene$^{\bullet+}$ and its derivatives in our previous studies, we suggest to assign this band to the CC stretching mode of the gauche conformer, which is calculated at 1549 cm^{-1}. This is probably the predominant contribution, however with a weak additional possible contribution from the combination $\nu_{14} + \nu_{17}$. While the intensity of the 1578 cm^{-1} band, relative to that of the 1622 cm^{-1} band, suggests that the s-trans conformer is the dominant form of the radical cation, one nevertheless has to conclude that the gauche conformer clearly is present at a relative concentration >10%. Considering the substantially higher energy (38.3−44.9 kJ mol^{-1}; see Table 1) calculated for the gauche than the s-trans conformer, a possible equilibrium between the two forms can be excluded, as it would be strongly biased toward the trans side. One thus has to conclude that the energy barrier between the two conformers is sufficiently high to prevent equilibration at room temperature within the lifetime (∼5 μs) of the radical cation. Having two minima on the potential energy surface, separated by an energy barrier E_a, the rate constant k for the process leading from one minimum to the other can be expressed as

$$k = (k_b T/h) \exp(-E_a/k_b T)$$

where k_b is the Boltzmann constant and h is Planck's constant. Since at 293 K, if at all, equilibrium is reached in a time which must be > 5 μs, E_a must be >42 kJ mol^{-1}, thus setting a lower limit for the torsional energy barrier between the two conformers.

Although the experimental RR spectrum could be assigned in a qualitative satisfactory way, we would like to add a few comments. As seen from the calculated spectra, calculated frequencies are very similar for many bands of the s-trans and gauche conformers. Some observed bands (e.g., that at 1043 cm^{-1}) may therefore contain contributions from both conformers. However, taking into account the low intensity of the observed 1578 cm^{-1} band, which, by analogy, is expected to be the strongest or one of the strongest bands of the gauche conformer, it is most likely that the relative contributions from the gauche conformer to the observed RR spectrum are minor.

While in previous experiments on the radical cation of butadiene and related compounds, the excitation wavelength was within the lowest allowed optical transition ($1^2A_u \leftarrow 1^2B_g$), in the present work the second transition ($2^2A_u \leftarrow 1^2B_g$) is the resonant one. It may therefore be of interest to qualitatively compare resonance Raman intensities for the two transitions. A comparison of the previously reported RR spectrum of the butadiene radical cation with that of TMB, presently reported, shows that while the totally symmetric CC stretching mode around 1600 cm^{-1} was the main mode observed with very high intensity in butadiene, in TMB an additional low-frequency mode (at 517 cm^{-1}) is strongly enhanced. This could be due either to methyl substitution or to different resonance conditions. As it seems unlikely that methyl substitution alone leads to the observed differences, we suggest that the observation of the 517 cm^{-1} mode is due to the different resonance conditions. As the displacements of the strongest enhanced modes reflect the geometry changes occurring upon excitation, this observation could be an indication that, for the lowest electronic transition, the main geometric distortion upon excitation is mainly a change in bond length of the CC bonds, while in the higher transition, an equally important deformation of bond angles takes place.

Furthermore, a comparison of the present RR spectrum of TMB$^{\bullet+}$ with that of the previously reported T_1 state of TMB[17] is of interest. If one compares observed vibrational frequencies of the two species, the close similarity of the two spectra is striking. As it seems highly unlikely that the T_1 state and radical cation have identical RR spectra, it seems that the RR spectrum,

previously assigned to the lowest triplet state of TMB, in fact was due to the radical cation. Previous experiments were carried out by sensitization with acetone in acetonitrile. An electron transfer process from TMB to acetone, excited to the T_1 state, may be the process responsible for the formation of the TMB radical cation in previous experiments.

Let us finally discuss the agreement between experimental and calculated frequencies from different methods. The applied scaling factors were obtained from the best fit procedure with experimental data. The scaling factors used for UHF, UB3LYP, and CASSCF methods are 0.89, 0.97 and 0.86, respectively. UBLYP frequencies are used without scaling. Compared with experimentally observed frequencies, the rms deviation obtained after scaling was 33.7, 12.2 (no scaling), 7.8, and 21.8 cm^{-1} for UHF, UBLYP, UB3LYP, and CASSCF. This suggests that the UBLYP method yields reasonably good results even without scaling, while after scaling by a factor 0.97, B3LYP gives the best vibrational frequencies compared with the experiment. As expected, the UHF method does not reproduce the vibrational frequencies very well due to the lack of electron correlation. CASSCF does better compared to UHF but not as good as DFT methods.

6. Summary and Conclusion

The structure of the radical cation of 2,5-dimethyl-2,4-hexadiene ($TMB^{\bullet+}$) was studied experimentally and theoretically. Experimentally, the time-resolved resonance Raman spectrum of the $TMB^{\bullet+}$ radical cation in aerated acetonitrile solution at room temperature was reported. The radical cation was generated by means of direct photoionization using 248 nm as pump wavelength and was probed at 360 nm, in resonance with the $2\ ^2A_u \leftarrow 1\ ^2B_g$ electronic transition. Theoretically, equilibrium geometries and harmonic force fields of neutral TMB and its radical cation were calculated and the optically observed transitions were assigned. The vibrational assignments of the observed resonance Raman spectrum were carried out with the help of calculated harmonic force fields obtained from different theoretical methods such as UHF, CASSCF, UBLYP, and UB3LYP procedures using 6-31G(d) as a basis set. Of the 21 bands observed in the 200−3000 cm^{-1} spectral region, 20 bands were assigned to fundamentals, overtones, and combinations of totally symmetric modes of s-*trans*-$TMB^{\bullet+}$. One remaining band was identified as due to the gauche conformer. DFT methods (UBLYP and UB3LYP) gave the best agreement with the observed Raman data. The present RR results suggest the presence of a small but significant amount of the considerably less stable gauche conformer of $TMB^{\bullet+}$ in solution at room temperature. A lower limit of 42 kJ mol^{-1} was estimated for the torsional energy barrier between the s-trans and gauche conformers.

Acknowledgment. This work was partially supported by a grant from the Danish Natural Science Research Council to the Center for molecular dynamics and Laser Chemistry. G.B gratefully acknowledges the above organization for their financial support.

References and Notes

(1) Shida, T. *Electronic Absorption Spectra of Radical Ions (Physical Sciences Data 34)*; Elsevier: Amsterdam, 1998.

(2) Lund, A., Shiotani, M., Eds. *Radical Ionic Systems, Properties in Condensed Phase*; Kluwer Academic Publishers: Dordrecht, 1991.

(3) Bally, T.; Roth, K.; Schrock, R. R.; Knoll, K.; Park, L. Y. *J. Am. Chem. Soc*. **1992**, *114*, 2440.

(4) Roth, H. D. *Photoinduced Electron-Transfer IV* **1992**, *163*, 131−254.

(5) Shida, T. *Annu. Rev. Phys. Chem*. **1991**, *42*, 55.

(6) Bally, T.; Nitsche, S.; Roth, K.; Haselbach, E. *J. Am. Chem. Soc*. **1984**, *106*, 3927.

(7) Hudson, B. S.; Kohler, B. E.; Schulten, K.; In *Excited States*; Lim, E., Ed.; Academic: New York, 1982; Vol. 6, pp 1−95.

(8) Turner, D. W.; Baker, C.; Baker, A. D.; Brundle, C. R.; *Molecular Photoelectron Spectroscopy*; Wiley-Interscience: New York, 1970.

(9) Koopmans, T. *Physica* **1937**, *1*, 104.

(10) Keszthelyi, T.; Wilbrandt, R.; Bally, T. *J. Mol. Struct*. **1997**, *410*, 339.

(11) Keszthelyi, T.; Wilbrandt, R.; Bally, T.; Roulin, J.-L. *J. Phys. Chem*. **1996**, *100*, 16850.

(12) Keszthelyi, T.; Wilbrandt, R.; Bally, T. *J. Phys. Chem*. **1996**, *100*, 16843.

(13) Keszthelyi, T.; Wilbrandt, R. *J. Phys. Chem*. **1996**, *100*, 15785.

(14) Keszthelyi, T.; Wilbrandt, R. *J. Mol. Struct*. **1996**, *379*, 211.

(15) Lew, C. S. Q.; Brisson, J. R.; Johnston, L. J.; *J. Org. Chem*. **1997**, *62*, 4047.

(16) Negri, F.; Orlandi, G.; Langkilde, F. W.; Wilbrandt, R. *J. Chem. Phys*. **1990**, *92*, 4907.

(17) Langkilde, F. W.; Wilbrandt, R. *Chem. Phys. Lett*. **1987**, *133*, 385.

(18) Abo Aly, M. M.; Baron, M. H.; Coulange, M. J.; Favort, J. *Spectrochim. Acta. A* **1986**, *42*, 411.

(19) Becke, A. D. *Phy. Rev. A* **1988**, *38*, 3098.

(20) Becke, A. D. *J. Chem. Phys*. **1993**, *98*, 5648.

(21) Lee, C.; Yang, W.; Parr, R. G. *Phys. Rev. B* **1998**, *37*, 785.

(22) Frisch, M. J.; Trucks, G. W.; Schlegel, H. B.; Gill, P. M. W.; Johnson, B. G.; Robb, M. A.; Cheeseman, J. R.; Keith, T.; Petersson, G. A.; Montgomery, J. A.; Raghavachari, K.; Al-Laham, M. A.; Zakrzewski, V. G.; Ortiz, J. V.; Foresman, J. B.; Cioslowsski, J.; Stefanov, B. B.; Nanayakkara, A.; Challacombe, M.; Peng, C. Y.; Ayala, P. Y.; Chen, W.; Wong, M. W.; Andres, J. L.; Replogle, E. S.; Gomperts, R.; Martin, R. L.; Fox, D. J.; Binkley, J. S.; Defrees, D. J.; Baker, J.; Stewart, J. P.; Head-Gordon, M.; Gonzalez, C.; Pople, J. A. *Gaussian 94*; Gaussian, Inc.: Pittsburgh, PA, 1995.

(23) Helgaker, T.; Jensen, H. J. Aa.; Jørgensen, P.; Olsen, J.; Ågren, H.; Andersen, T.; Bak, K. L.; Bakken, V.; Christiansen, O.; Dahle, P.; Dalskov, E. K.; Enevoldsen, T.; Fernandez, B.; Heiberg, H.; Hettema, H.; Jonsson, D.; Kirpekar, S.; Kobayashi, R.; Koch, H.; Mikkelsen, K. V.; Norman, P.; Packer, M. J.; Saue, T.; Taylor, P. R.; Vahtras, O. *DALTON*, an electronic structure program.

(24) Gorman, A. A.; Gould, I. R.; Hamblett, I. *J. Am. Chem. Soc*. **1981**, *103*, 4553.

(25) Gorman, A. A.; Gould, I. R.; Hamblett, I. *J. Photochem*. **1982**, *19*, 89.

(26) Caldwell, R. A.; Singh, M. *J. Am. Chem. Soc*. **1982**, *104*, 1621.

(27) Kumar, C. V.; Chattopadhyay, S. K.; Das, P. K. *Chem. Phys. Lett*. **1984**, *106*, 431.

(28) Mohandas, P.; Umapathy, S. *J. Phys. Chem*. **1997**, *101*, 4449.